Joule

CellPress

Perspective

Transparent Polymer Photovoltaics for Solar Energy Harvesting and Beyond

Sheng-Yung Chang,[1] Pei Cheng,[1] Gang Li,[2] and Yang Yang[1,*]

Polymer photovoltaics have become a promising alternative energy due to lightweight properties, environmental friendliness, and solution processability. Transparent organic photovoltaics in particular have been recently receiving more attention in the photovoltaics field due to their unique potential in future applications beyond mere harvesting of solar energy. This perspective is further enhanced by the recent developments of high-performance polymer photovoltaics (including infrared absorbing materials and devices) that could achieve superior visible transparency and power conversion efficiency. To realize high-performance transparent organic photovoltaics, the main strategy is to shift the active-layer absorption spectrum to the infrared region by designing new low-bandgap donors and non-fullerene acceptors, and to reduce the invalid absorption by developing new transparent electrode materials. The potential applications are diverse, especially for spectrum-sensitive ones such as the greenhouse in agriculture. Finally, some key research areas of transparent organic photovoltaics that may deserve further attention are discussed.

Introduction

Harvesting energy from the sun is attracting increasing attention due to the challenges arising from our continued dependence on fossil fuels. In the past two decades, polymer photovoltaics (PV) based on bulk-heterojunction (BHJ) structure have become a promising alternative energy option due to their lightweight properties, environmental friendliness, and solution processability.[1–5] The capability for solution processing especially provides the possibility of fabricating organic devices on flexible substrates and over large device areas with relatively simple equipment and low costs. The certified power conversion efficiency (PCE) of organic PV (OPV) has already exceeded 12% by a combination of novel materials and morphology optimization.[6,7]

Due to the nature of molecular orbitals, the absorption spectra of organic semiconductors are not continuous as in inorganic semiconductors. This results in a major shortcoming for single-junction polymer PV devices in terms of their insufficient light absorption. However, this "disadvantage" of polymer PV can actually open a door to a new opportunity: visible region transparency. The active layer in a transparent organic photovoltaics (TOPV) device is required to exhibit high transparency in the visible region. In this article, to simplify the conditions in different optical transparencies, we use "TOPV" to represent transparent, semi-transparent, and translucent OPV. According to the energy distribution of the AM 1.5G solar spectrum, 51% of the solar energy is distributed within the infrared (IR) region (shown in Figure 1A).[8] As a result, the theoretical PCE of polymer PV with only IR absorption is able to be as high as the device with only visible absorption, or even better.

Context & Scale

Polymer photovoltaics are a promising alternative energy for visible-spectrum applications because the absorption spectra of organic semiconductors, including polymer and small-molecule types, are not continuous as in inorganic semiconductors. As a result, the design of organic materials is able to pass visible light and absorb non-visible light such as the infrared. According to the energy distribution of the solar spectrum, more than a half of solar light is distributed within the infrared region. The theoretical efficiency of polymer photovoltaics with only infrared absorption therefore can be as high as a device with only visible absorption. Accordingly, we present a perspective that concisely reviews the developments in transparent polymer photovoltaics and their potential applications in order to engender new ideas on achieving superior transparency, power conversion efficiency, and more practical utilities.

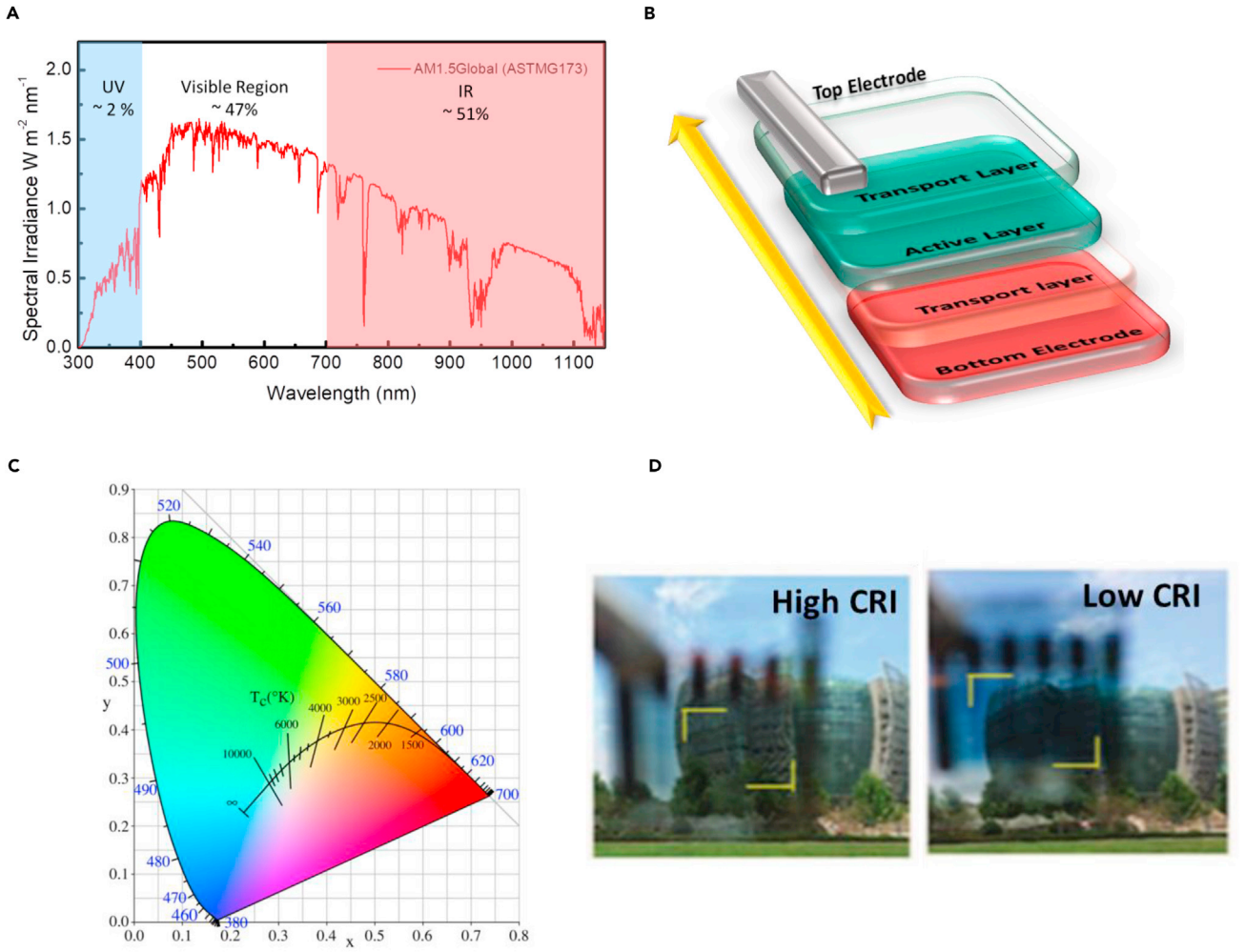

Figure 1. Schematic of Transparent Polymer Photovoltaics

(A) The solar emission spectrum and the energy proportion in different regions is indicated.[8]

(B) Schematic of a typical transparent organic photovoltaic device.

(C) CIE 1931 color space.

(D) Comparison of photos with high and low CRI values, showing the view through transparent organic photovoltaic modules.[9] Reprinted from Xu et al.,[9] with permission. Copyright 2017, Wiley-VCH.

Although intensive attention has been paid to OPV since the 1990s, the potential of TOPV was not realized until 2006.[10,11] The typical TOPV device is shown in Figure 1B. In the last decade, the progress in TOPV development was relatively slow due to the low PCE. Recently, because of the rapid developments of novel and visibly transparent semiconductors and electrodes, important studies on different aspects of TOPV have been carried out. Herein, we present a review perspective on the developments of TOPV devices and their potential applications, with a goal of inspiring new ideas that could achieve superior transparency and PCE.

Physical Properties

To compare the performance of the TOPV (excluding PCE), it is essential to evaluate three major device properties: absorption region, average visible transmittance (AVT), and color-rendering index (CRI).[12,13]

[1]Department of Material Science and Engineering, University of California, Los Angeles, CA 90095, USA

[2]Department of Electronic and Information Engineering, The Hong Kong Polytechnic University, Hung Hom, Kowloon, Hong Kong, China

*Correspondence: yangy@ucla.edu

https://doi.org/10.1016/j.joule.2018.04.005

Absorption Region

To achieve IR absorption of the OPV, reducing the band gap between the lowest-energy unoccupied molecular orbital (LUMO) and the highest-energy occupied molecular orbital (HOMO) is required. To reduce the bandgap of organic materials, the general approach is to decrease the bond length alternation (BLA) value, which is the average of the difference in length between adjacent carbon-carbon bonds in a polyene chain.[14,15] As the quinoid contribution in the polymer chain is raised, such as forming a mesomeric structure, the carbon-carbon single bonds between two adjacent rings can adopt more double-bond characteristics and the BLA begins to decrease. The other useful way to decrease the BLA is to incorporate conjugated electron-rich donor (D) units and conjugated electron-deficient acceptor (A) units together in the same polymer backbone, which generate a strong push-pull driving force and, thus, enhance electron delocalization.[16,17] Based on the D-A structure, strengthening one of the donor units, acceptor units, or both of them in the same polymer backbone can further reduce the bandgap. Additionally, enhancing the intermolecular conjugation, such as strengthening planarization between adjacent aromatic units by forming additional covalent or non-covalent bonds, can also decrease the BLA by inducing parallel p-orbital interactions that extend conjugation and facilitate delocalization.[18]

Average Visible Transmittance

The visible spectrum is from 380 to 760 nm, which corresponds to wavelengths of the incident photons that can be perceived by the naked human eye. The AVT can be expressed as a summation of transmission spectrum (T), incident light flux (F), and human eye photonic response (E) divided by F times E[19]:

$$\frac{\int T(\lambda)F(\lambda)E(\lambda)d\lambda}{\int F(\lambda)E(\lambda)d\lambda}$$

The balance between AVT and absorption within visible region should be carefully considered. To minimize the unnecessary absorbance from layers other than the photoactive one, the thickness of the traditional metal electrode should be reduced or, alternatively, a novel conductive material such as graphene should be used as an electrode.

Color-Rendering Index

For a TOPV that is used in human vision-related applications, the precision of demonstrated color should also be taken into consideration. To examine the color quality of the TOPV, the Commission Internationale d'Eclairage (CIE) 1931 color space (shown in Figure 1C) is used as a standard as it can quantitatively define pure physical colors of the visible spectrum perceived by human eyes. The standard daylight illuminant D65 or AM 1.5G solar spectra are often used as references for evaluating the color neutrality of the device of interest. If the color coordinate (x, y) of the PV device under illumination is closer to the white light region defined by CIE 1931 chromaticity coordinate, the PV device is more suitable for window use or human vision applications because of a better color neutrality.[20] To further numerically compare the color difference between the color of the original source and the transmitted one, the CRI is used on a scale from 0 to 100. As shown in Figure 1D, an object with a higher CRI means it displays more neutral and real color closer to how the original light source does.[9] One of the strategies that can be used to increase the CRI of the device is to modulate the light coupling by using a sandwiched structure of dielectric materials/metal and low-bandgap photoactive materials. The related work is further discussed and elaborated in the following sections.

Table 1. Materials Used for the Infrared and Transparent Organic Photovoltaic Devices

Device Structure	Transport Layer + Back Electrode	Absorption (nm)[a]			Device Efficiency			AVT (%)	CRI	Reference
		Peak	Cutoff	V_{OC}	J_{SC}	FF	PCE			
PBDTT-DPP:$PC_{61}BM$	AgNW	770	850	0.77	9.3	56.2	4.0	61.0	–	21
PDTP-DFBT:$PC_{71}BM$	Ca/Al	800	900	0.70	18.0	63.4	8.0	–	–	22
PDPP4T-2F:$PC_{71}BM$	MoO_3/Al	800	900	0.79	15.9	65.8	8.2	–	–	23
PBDTT-SeDPP:$PC_{61}BM$/	TiO_2/AgNW	810	900	0.73	10.9	58.0	4.6	63.0	–	24
PDPPSDTPS:$PC_{61}BM$	MoO_3/Ag	900	1,100	0.35	16.7	52.0	3.1	–	–	25
PDPPTDTPT:$PC_{61}BM$	MoO_3/Ag	880	1,000	0.45	17.3	57.0	4.4			25
PTB7-Th:ITIC	TiO_2/AgNW	720	780	0.81	14.2	59.1	6.8	–	–	26
PTB7-Th:IHIC	MoO_3/Au(1)[b]/Ag(15)	820	900	0.75	19.0	68.1	9.8	36.0	–	27
PBDTTT-E-T:IEICO	PFN-Br/Al	810	925	0.82	17.7	58.0	8.4	–	–	28
PTB7-Th:IEICO-4F	PFN-Br/Al	870	1,000	0.74	22.8	59.4	10.0	–	–	29
P3HT:$PC_{61}BM$	M-PEDOT:PSS/ITO	–	–	0.56	9.7	–	–	~70	–	30
PCPDTFBT:$PC_{71}BM$	M-PEDOT:PSS/Ag(10)	–	–	0.74	11.4	58.6	5.0	47.3	–	31
pDPP5T-2:$PC_{61}BM$	ZnO/AgNW	700	850	0.56	8.5	60.2	2.9	41.0	–	32
PTB7:$PC_{71}BM$	BCP/PC-thin-Ag(10)			0.72	10.7	68.0	5.2	29.0	–	33
PIDT-PhanQ:$PC_{71}BM$	surfactant/Ag(10)			0.79	5.8	57.0	2.6	31.7	–	34
PSBTBT:$PC_{71}BM$	$LiCoO_2$/Al/ZnO:Al	–	–	0.61	10.7	42.0	2.8	–	83	35
PBDTTT-C-T:$PC_{71}BM$/	MoO_3/Ag(6)	–	–	0.75	9.3	61.0	4.3	35.9	96	36
PCDTBT:$PC_{71}BM$	WO_3/Ag/1DPC	–	–	0.87	9.6	63.1	5.3	25.1	97	37

FF, fill factor.

[a]"Absorption" refers to the absorption properties of the active layer.

[b]The number in parentheses refers to the thickness of the metal.

Transparent Devices: Photoactive Materials

Polymer Donors

The materials that have been facilitated or are potential for transparent photovoltaics are listed in Table 1. In the first place, polymer-type materials will be introduced. Some of the visibly transparent organic polymers that are more commonly used as a donor are shown in Figure 2A. Diketopyrrolopyrrole (DPP) is a red pigment widely used in inks, electroluminescent devices, and transistors. It has a conjugated structure with strong π-π interactions.[38] Moreover, its lactam group has strong electron-withdrawing effect, which leads to overall high electron affinity of DPP. As a result, LUMO and HOMO energy levels of DPP lie relatively lower, making DPP an ideal acceptor unit for visibly transparent materials.[39] Based on this unit, Huo et al. synthesized a series of DPP-based polymers for harvesting photons in the near-IR region.[40] To improve the previous low-bandgap polymer design for a higher performance, the polymer PBDTT-DPP was proposed.[41] Its thienylbenzodithiophene (BDTT) unit, which replaces the oxygen atoms attached to the benzodithiophene unit with thiophene moieties, lowers the HOMO and LUMO energy levels.[42] This is a weak donor-strong acceptor design, which is preferable to balance the needs for both the small bandgap and large open-circuit voltage (V_{OC}) of a PV device. This design increases the V_{OC} without compromising the driving force for exciton separation. Its optical bandgap is 1.44 eV and its absorbance profile is shifted to the near-IR region, leading to an absorption peak at around 770 nm and relatively low absorbance from 400 to 650 nm. The efficiencies of PBDTT-DPP-based transparent devices with indium tin oxide (ITO) and silver nanowire electrodes (as shown in Figure 3A) were measured to be 4.0% and 3.8% when shone upon from anode and cathode side, respectively. The device transparency in the visible region

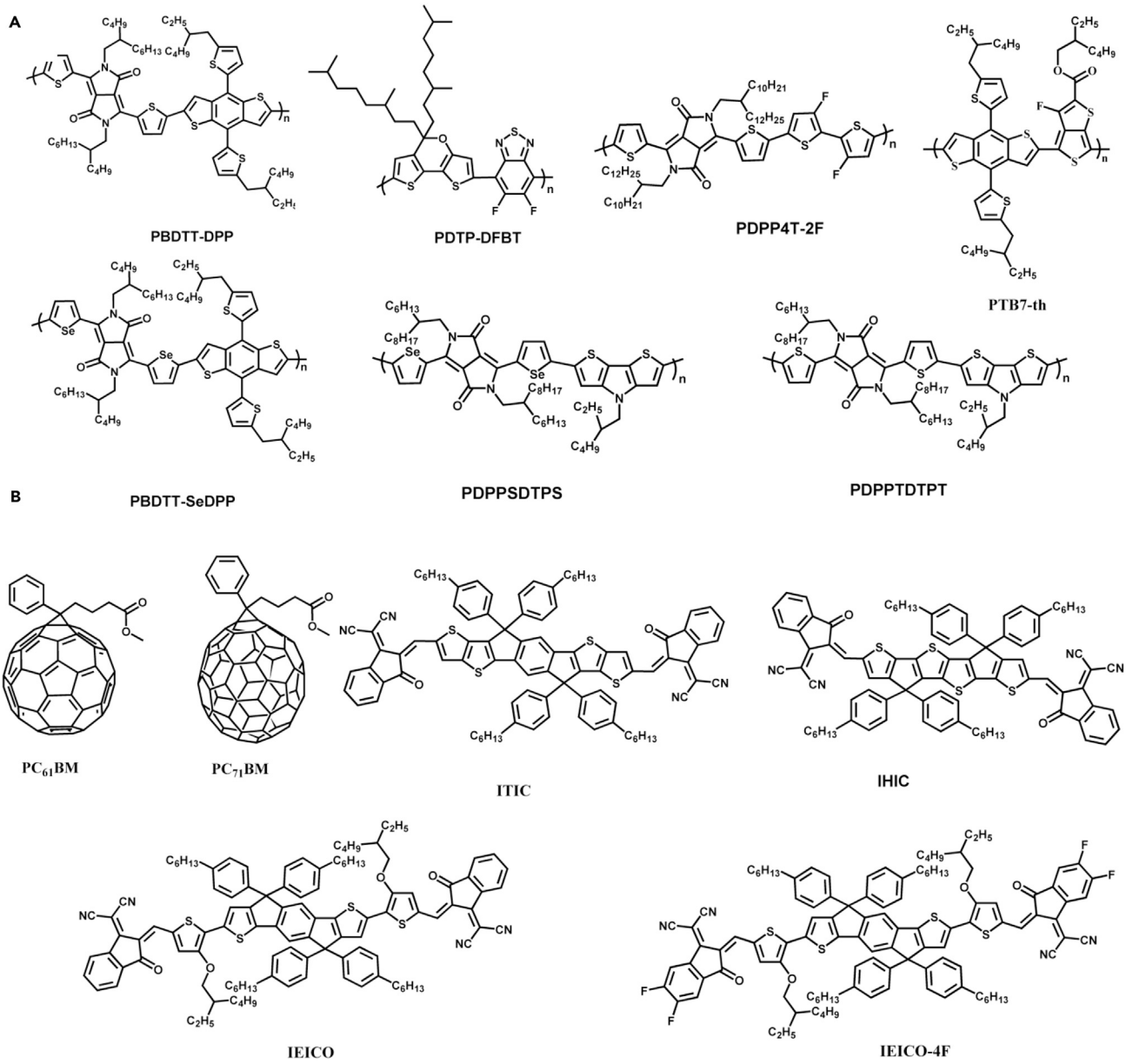

Figure 2. Organic Materials for Transparent Polymer Photovoltaics

(A and B) Polymer donors (A) and small-molecular acceptors (B) for transparent organic photovoltaic devices.

was on 61% on average.[21] To further improve the efficiency of this polymer and push the absorption into the IR region, selenium is a reasonable option for substituting the atom in the acceptor unit. It has a stronger heteroaromatic interaction than sulfur due to its larger size, which enhances the interchain interaction as well as the charge transport.[43-45] Hence, it was shown that the polymer PBDTT-SeDPP, which substitutes the sulfur atom on the thiophene moiety of PBDTT-DPP by a selenium atom, lowers the bandgap and increases the charge carrier mobility.[46] Its absorption cutoff and the maximum peak value were red-shifted by 50 nm compared with the ones of the PBDTT-DPP. By applying PBDTT-SeDPP:$PC_{61}BM$ to the transparent device structure, a PCE of 4.6% (average 4.1%) and an average light transmission of 63% were achieved.[24]

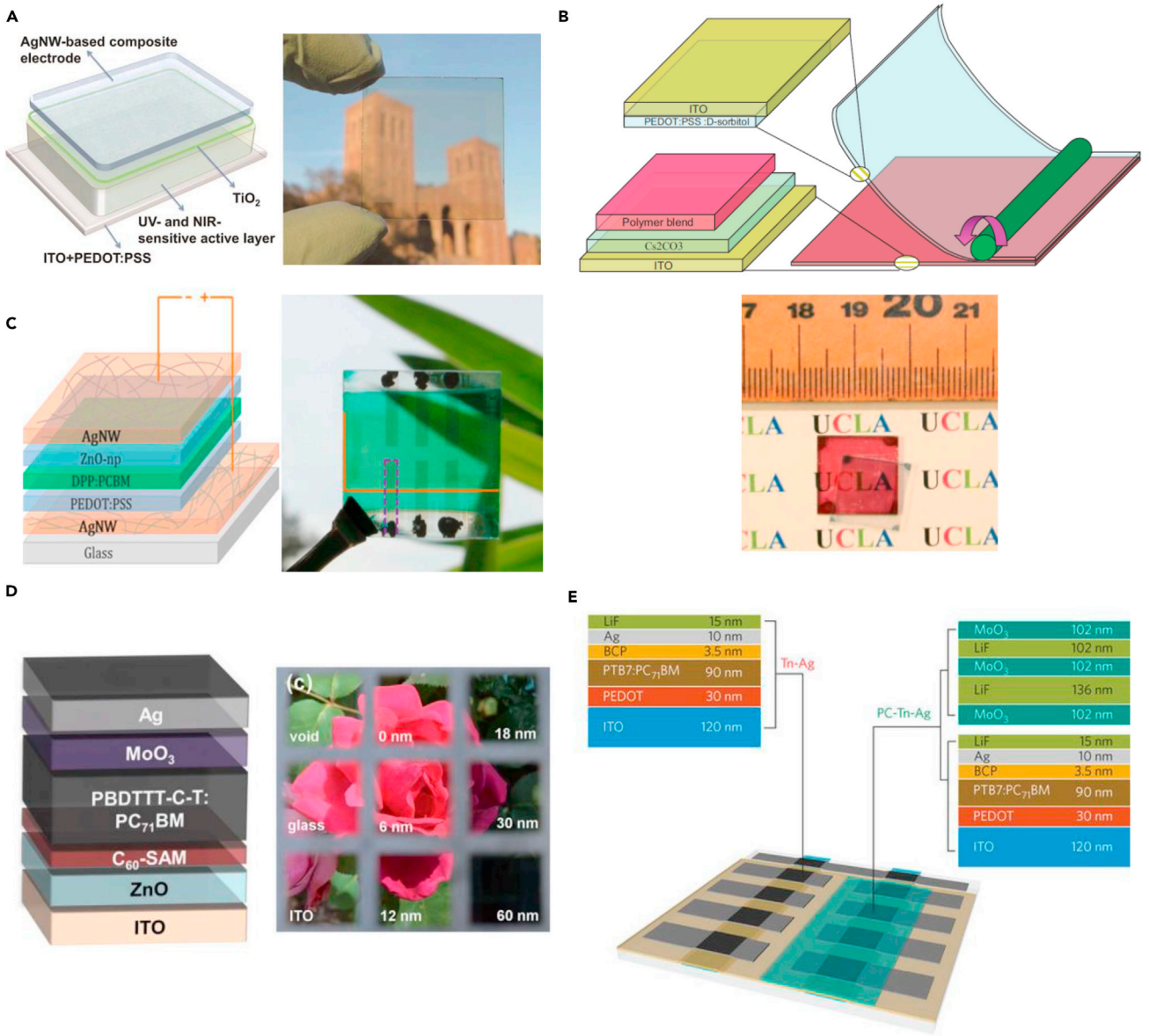

Figure 3. Selected Works of Transparent Polymer Photovoltaics

(A) (Left) Schematic of the device architecture for ITO-AgNW transparent photovoltaics. (Right) Demonstration of the actual device. Reprinted from Chen et al.,[21] with permission. Copyright 2012, American Chemical Society.

(B) (Upper) Schematic for the ITO-ITO transparent photovoltaics. (Lower) Demonstration of the actual device. Reprinted from Huang et al.,[30] with permission. Copyright 2008, Wiley-VCH.

(C) (Left) Architecture of AgNW-AgNW transparent photovoltaics. (Right) Demonstration of the actual device. The rectangular areas bound by the orange solid line and purple dashed line indicate the top and bottom of the AgNW electrode, respectively. Reprinted from Guo et al.,[32] with permission. Copyright 2014, American Chemical Society.

(D) (Left) Architecture of ITO-Ag transparent photovoltaics. (Right) Photographs taken through devices with the six different Ag thicknesses and blank ITO and glass substrates. Reprinted from Chen et al.,[36] with permission. Copyright 2012, Royal Society of Chemistry.

(E) The view of ITO-photonic layer transparent photovoltaics. Reprinted from Betancur et al.,[33] with permission. Copyright 2013, Nature Publishing Group.

A good polymer PV device usually carries good crystalline properties suitable for favorable phase separation of the donor and acceptor aggregate.[47–49] To have good crystalline morphology while maintaining the capability for solution processing, a polymer design of PDPP4T was proposed, which has one DPP unit and four thiophene groups

as electron-donating units in its backbone, as well as long alkyl chains attached to DPP unit for obtaining excellent solubility.[50] Zheng et al. further improved the structure to be PDPP4T-2F, which substitutes the hydrogen atoms attached to two end-group thiophenes by fluorine atoms, making the absorption onset shift to 900 nm and lowering the HOMO and LUMO levels to −5.2 eV and −3.7 eV.[23] Grazing incidence wide-angle X-ray scattering measurement patterns and temperature-dependent absorption spectra also showed that PDPP4T-2F has stronger intermolecular π-π interaction than that of the PDPP4T. This is due to larger intermolecular aggregation, which can explain the red-shift and a higher mobility of PDPP4T-2F. The resulting optimized performance of an opaque PDPP4T-2F-based device is 8.2%.

In addition to the weak donor-strong acceptor design, several research groups also facilitated a strong donor-strong acceptor structure. Dou et al. incorporated three strong electron-donating groups including dithienopyran (DTP), cyclopentadithiophene (CPDT), and benzodithiophene (BDT) into an IR low-bandgap polymer.[22,51] DTP is measured to have the highest HOMO level (−5.2 eV, compared with −5.3 eV for CPDT and −5.4 eV for BDT) due to the strongly electron-donating oxygen atom in its pyran ring. By combining DTP unit into a strongly electron-withdrawing difluorobenzothiadiazole (DFBT) unit, the absorption onset of the polymer is located at around 890 nm. The bandgap is calculated to be 1.38 eV, which is the smallest value among the three polymers. The small-energy bandgap can be ascribed to the enhanced intramolecular charge transfer between the strongly electron-donating and strongly electron-withdrawing interaction. The absorbance is mainly focused from 600 to 900 nm and, hence, the visible region is rather transparent. The highest PCE of the PDTP-DFBT:$PC_{71}BM$ device is 8.0% with a V_{OC} of 0.7 V, which shows a decent V_{OC} loss value.

To push the absorbance further into the IR region, the bandgap could be decreased; hence to this end, Hendriks et al. combined DPP moieties alternating with very strong electron-donating pyrrole-based groups to make IR polymers.[25] Two sequential processes for synthesis are taken. In the first process, N-methylpyrrole is chosen as an electron donor and the pyrrole is replaced by an even stronger donor, dithienopyrrole, which selectively increases the HOMO energy level. The resulting co-polymer PDPPTDTPT decreases the optical bandgap from 1.3 to 1.2 eV. In the second process, thiophene-to-selenophene substitution on the DPP is selected to raise the HOMO energy level selectively. The product, PDPPSDTPS, ultimately shrinks the optical bandgap from 1.3 to 1.1 eV. The resulting polymers show LUMO levels at about −3.7 eV, which remain unchanged throughout the processes. This value is suitable to have enough energy difference for electron separation between the LUMO levels of the polymers and PCBM ([6,6]-phenyl-C61-butyric acid methyl ester). In an inverted structure device, the external quantum efficiency (EQE) values of both polymers within 400–600 nm are all below 40% with strong near-IR contribution. The EQE peaks of both PDPPTDTPT and PDPPSDTPS are located at around 900 nm and the cutoffs extend to 1,100 and 1,200 nm, respectively. Specifically for PDPPSDTPS, there is still 50% EQE at 1,000 nm. The final device PCE reaches 4.4% for PDPPTDTPT and 3.1% for PDPPSDTPS.

Small-Molecular Acceptors

As one of the most successful acceptor materials, fullerene and its derivatives dominate the TOPV research interests because of their easy processability and efficient electron transport properties. However, further modification of energy levels of fullerene-based materials is limited by their buckyball structure, and their absorption spectra can scarcely be tuned. To design new acceptor materials with near-IR

absorption, several synthesis strategies providing decent transport properties and energy shift can be considered. For instance, aromatic fused rings have the extended conjugation in fused rings, which is advantageous due to more effective interchain π-π interactions and enhanced intermolecular charge transport. The introduction of electron-withdrawing moieties works for designing acceptor materials in a similar fashion.

Therefore, in Figure 2B we list several commonly preferred small molecules serving as low-bandgap acceptors. For a fused ring-based acceptor for heterojunction OPV, the planarity and aggregation ability should be carefully designed. Lin et al. synthesize ITIC, which contains a seven-ring fused core indacenodithieno[3,2-b]thiophene (IT) end-capped with 2-(3-oxo-2,3-dihydroinden-1-ylidene)malononitrile (INCN) groups, with four 4-hexylphenyl groups substituted on the IT group.[26] One carbonyl and two cyano groups on the INCN have strong electron-withdrawing ability and, thus, lower the LUMO levels. The resulting push-pull structure shows a better intramolecular charge transfer and extends absorption further than that of fullerene derivatives. The absorption of the ITIC film has a strong shoulder peak, implying the strengthened molecular self-organization and π-π stacking. The optical bandgap of ITIC film is 1.6 eV and the absorption cutoff is 780 nm. The HOMO and LUMO energy levels are estimated to be −5.5 and −3.8 eV, respectively, from the onset oxidation and reduction potentials. When incorporated with a relatively low-bandgap donor polymer PTB7-Th,[52] the maximum device PCE is 6.8%. A single heterojunction containing ITIC can achieve more than 11% PCE.[53] ITIC reveals the possibility to achieve high efficiency via a non-fullerene acceptor and low-bandgap donors, opening a synthesis route for the series of derivatives. In addition, there are other methods to extend the absorption of the ITIC to longer wavelength region, such as introducing double-bond π-bridge between its D and A units to minimize the bandgap. Incorporating fluorine substituents on acceptor end groups can further lower the energy levels.[54,55] Huang et al. reported a near-IR small-molecular ITVfIC by facilitating these strategies for high-efficiency TOPV.[56] The PTB7-Th:ITVfIC device with a 15-nm silver electrode can achieve a PCE of 8.2% with a 40.5% AVT.

One of the other electron-donating molecules commonly used is indacenodithiophene (IDT), which has good planarity. Further replacement of the central phenyl unit of IDT with thieno[3,2-b]thiophene enhances its electron-donating ability. The increased size and planarity of the monomer unit, as well as the intermolecular S-S interactions, strengthen the π-π stacking of polymer chains. This prevents rotational disorder, reduces the energy of reorganization, and enhances charge hopping and consequently charge carrier mobility, which overall makes IDT a strong candidate for PV.[57] Based on this unit, Wang et al. designed a near-IR non-fullerene acceptor, IHIC.[27] IHIC was synthesized by flanking INCN groups to the IDT unit inducing strong intramolecular charge transfer and shifts of its absorption spectrum into the near-IR region. The thin film of IHIC shows strong absorption within the 600- to 900-nm range and an optical bandgap of 1.38 eV. The HOMO and LUMO energy levels of IHIC are estimated to be −5.5 and −3.9 eV, respectively, which are suitable for a good acceptor for transparent OPV. Based on a blend of a relatively low-bandgap polymer donor PTB7-Th and IHIC, the device PCE reaches 9.8% with an AVT of 36%. Furthermore, Lin et al. combined IDT with INCN groups, with a CHO unit as π-bridges, to obtain another near-IR material named IEIC.[58] IEIC exhibits strong absorption spectrum from 500 to 800 nm with an optical bandgap of 1.5 eV. To enhance its absorption into the IR region, Yao et al. introduced alkoxy groups onto IEIC to yield an IR acceptor named IEICO.[28] The alkoxy group raises selectively the HOMO level by 0.2 eV with little change in LUMO level compared

with the original IEIC. The absorption spectrum of the thin film of IEICO red-shifts by 90 nm compared with IEIC. When combined with a conjugated polymer PBDTTT-E-T, which has an absorption spectrum complementary to IEICO, the highest device PCE reaches 8.4%. In addition to adding alkoxy groups on the donor moieties, introduction of fluorine atoms into its acceptor moieties further strengthens the ICT effect.[29] The resulting non-fullerene acceptor IEICO-4F red-shifts the absorption spectrum by approximately 200 nm and the LUMO of IEICO-4F is lowered by 0.2 eV to an energy level of – 4.2 eV. Its optical bandgap was measured to be 1.24 eV, showing an absorption cutoff at 1,000 nm. When combined with the PTB7-Th into a heterojunction device, a PCE of 10.0% and a short-circuit current density (J_{SC}) of 22.8 mA cm^{-2} is achieved, for which the energy loss, 0.5 eV, is impressive. These design strategies for IEIC are proven as successful, and the derivatives are competitive candidates for applications in TOPV.

Li et. al synthesized BT-CIC, which comprises four chlorine (Cl) atoms at the INCN end groups linked to the a strong electron-donating benzodithiophene (BT) unit.[59] The Cl atoms can also lower the bandgap by enhancing intramolecular charge transfer and intermolecular interactions of chlorine between chlorine atoms that are between the sulfide lead in well-ordered molecular stacking for the donor-acceptor blend. The bandgap was about 1.3 eV and its absorption cutoff was 950 nm. Its opaque PV devices with PTB7-Th yield a PCE of 11.2% and a J_{SC} of 22.5 mA cm^{-2}. When reducing its silver electrode thickness to 10 nm, the device AVT was able to reach 43% and CRI of 91 while maintaining a PCE of 7.1%.

Transparent Devices: Electrode Materials

Another important research focus in TOPV is on the electrode. The common material for electrodes is a metal with a thickness of more than 100 nm. The high thickness for better electronic conductivity and more reflected photons of the PV device will inevitably make the final device opaque. To date, several remarkable studies of advanced transparent electrodes have been conducted in order to achieve a more efficient TOPV.[60]

One widely used electrode is ITO, which has both good transparency and conductivity. Hence, it is a strong candidate for the applications in TOPV. Huang et al. studied ITO performance as a transparent electrode. They used it in a device with PEDOT:PSS of high work function as a hole-transporting layer and solution-processable buffer layers, such as Ca_2CO_3, of low function as an electron-transporting layer (as shown in Figure 3B).[30] The PEDOT:PSS also served as an electronic "glue" to connect the two subcells together by exerting forces on them. It was found that the buffer layers containing the same metal ion show similar work function values and the coated Cs-containing salt buffer layers reduce the work function of ITO the most. This is because the dipole moment is directly related to the electron-donating ability of metal species and also the ITO surface with the O-Cs dipole layer. It has the lowest effective work function owing to the highest dipole moment among all of the chosen materials. The formation of the dipole layer enhanced interfacial charge transfer rate and caused higher J_{SC} and lower resistance. In the other case, Chang et al. used ITO and ultra-thin silver as the transparent cathode and anode, respectively, in a low-bandgap polymer PCPDTFBT system, for which the absorption cutoff was 900 nm.[31] The PEDOT:PSS layer was used to provide good wettability for silver atoms when depositing, which reduced the surface roughness of the overlying silver.[61] The device PCE reached 5.0% with an AVT of 47.3% with a 10-nm silver thickness.

Nonetheless, it is estimated that the deposition of ITO on flexible substrates accounts for 90% of the total energy required in the polymer PV manufacturing process.[62] Selecting an electrode for an ITO-free and fully solution-processed OPV is challenging due to several requirements. For example, the bandgap of an ITO-free electrode cannot be reduced when compared with the one made of ITO. Due to the high conductivity of a metal, it is also possible to prepare an ultra-thin silver layer or silver-based material combinations for good electrodes. Based on this concept, Guo et al. facilitated silver nanowire (AgNW) electrodes as both anode and cathode in a DPP-based low-bandgap polymer pDPP5T-2 and $PC_{61}BM$ system (as shown in Figure 3C).[32] The PEDOT:PSS layer was introduced between the photoactive and the bottom AgNW layer and the ZnO layer between the top AgNW and photoactive layer electrodes. This design improved the surface contact without compromising transparency and resulted in transparent devices with a PCE of 2.9% and AVT of 41% in the 400- to 800-nm region.

It was also discovered that combining silver with other chemical compounds can fine-tune the transport property. Hence, Chueh et al. reported a TOPV using ultra-thin silver with fullerene-containing surfactant as electrode in a PIDT-PhanQ:$PC_{71}BM$ system.[34] This hybrid electrode can serve as an optical spacer to spatially redistribute the light intensity within the device and also provide a preferential interface for the electron transport between organic and metal layers. Upon decreasing the thickness of silver from 50 to 10 nm, increased the device performance from 13% to 30% while the PCE reached 5.1% with a corresponding AVT of ~25%. To further examine the influence of the silver thickness on other optical properties, Chen et al. used thin silver layers as electrode in a PBDTTT-C-T:$PC_{71}BM$ system.[36] By tuning the thickness of the silver layer from 60 nm to 6 nm, they were able to control the balance between the device performance and transparency. The most transparent device in this work reached a 4.3% PCE with a 36% AVT. It was found that by using a silver layer with a thickness of less than 30 nm, the color coordinates of the OPV device were located in a relatively white area in the CIE 1931 diagram under AM 1.5G illumination, and thus emitted a neutral color for the human eye. As shown in Figure 3D, the devices with 12- and 18-nm silver electrodes are the closest to the standard daylight illuminant point. The general CRI of all devices was higher than 96, and hence this work provides an example of a polymer PV that could be used in windows while maintaining high efficiency.

The dielectric-metal-dielectric structures are reported to have superior transparency, good conductivity, and easy-to-tune work function. They also have excellent mechanical flexibility that is advantageous for flexible PV.[63] Colsmann et al. reported using an $LiCoO_2$/Al/ZnO:Al cathode in a PSBTBT:$PC_{71}BM$ system to achieve a TOPV with good color display ability.[35] The device PCE was measured to be 2.8%, while an 83% CRI value from transmitted AM 1.5G light source and 86% from standard illuminant A source were achieved. These results demonstrated a neutral color perception and good color-rendering properties.

To collect photons in the TOPV more efficiently, the photonic crystal structure can be introduced. This structure is made by combining a low-refractive-index material layer with a high-refractive-index one to form a periodic array, which can selectively reflect the photons at a specific region of the photon spectrum and strengthen the reflection by enhanced interference. As shown in Figure 3E, Betancur et al. proposed to construct a 1D photonic crystal (1DPC) array after depositing an ultra-thin silver layer so that it could serve as a mirror for near-IR (>650 nm) and near-UV (<450 nm) photons.[33] For this study, they chose lithium fluoride (LiF) as a low-

refractive-index material and molybdenum trioxide (MoO_3) as a high-refractive-index material. Based on a PTB-7:$PC_{71}BM$ system, the J_{SC} of the transparent device was 63.8% of the opaque one, while the J_{SC} for the five-layered photonic crystal array device was 76.3%. The PCE of the device with photonic crystal and thin silver electrode reached 5.6% and the transparency in the visible was close to 30%. Yu et al. deposited 1DPC layers onto the thin silver layer to analyze the differences in optical properties of multiple-layer devices.[37] When the number of overall 1DPC layers in a PCDTBT:$PC_{71}BM$ system increased from 0 to 5, the AVT of the device decreased from 28.4% to 25.1% due to the reflectance of the photonic crystal. Hence, it can be inferred that the device PCE could be higher than 5% with more than one layer of 1DPC. Higher number of 1DPC layers could also provide a more neutral color in CIE 1931 and CIE 1960 diagrams. The CRI of five layers of 1DPC is 97% and the three and four pairs show a CRI value higher than 90%. These research achievements of photonic crystal layers provide a promising way to distribute the inner light field more effectively across the device and thus lead to more precise colors in human vision applications.

Applications

A Light Intensity-Sensitive Case

The transparent PV module can be integrated into several important fields, ranging from indoor sensors for the Internet of Things to building-integrated photovoltaics (BIPV).[13] Indoor applications usually operate at low illuminance and consume very low power. In contrast, BIPV is designed to incorporate into or replace traditional roofs and windows to absorb the outdoor sunlight and supply additional power to the building. For the former application, TOPV have advantages over the inorganic counterpart under indoor light (0.002–0.003 sun, 300–500 lux) conditions. Organic material has much higher light extinction coefficient and lower dependence of V_{OC} on illuminance. As a result, the device efficiency degradation from outdoor 0.1–0.5 sun (12,000–60,000 lux) to indoor light intensity is much lower for the organic module.[64,65] Besides, the better capability to be embedded into curved or flexible substrates due to the thinner photoactive layer also makes organic devices more applicable in a wide range of short-life-cycle electronics.

A Spectrum-Sensitive Case

Among all potential outdoor applications, utilizing TOPV in BIPV in greenhouses for agricultural applications (as shown in Figure 4A) has more obvious advantages over the traditional module due to the ability of spectrum control.[66–72]

Agricultural plants utilize specialized pigments to intercept and capture photon energy for growth. Within the broad solar light spectrum, as shown in Figure 4B, the photosynthetically active radiation (PAR) activates the chlorophyll *a* and *b* pigments, transforming light energy into chemical energy for production of carbon molecules (such as sugars) within 400–700 nm. The products are then used to construct more complex compounds, and ultimately plant cells and organs such as roots, leafs, stems, flowers, and fruits.[73] In addition to providing energy for plant photosynthesis, light within specific regions also regulates the plant growth. This process is called photomorphogenesis, involving the activation of several photoreceptor (pigment) systems. Plants use primarily blue light for vegetative leaf growth and red light for flowering, for instance.[74]

There is also an obvious difference in light intensity requirements for crops versus biomass/algae growth. For instance, crops typically prefer high light intensity, while algae require light with much lower intensity. It was found that the

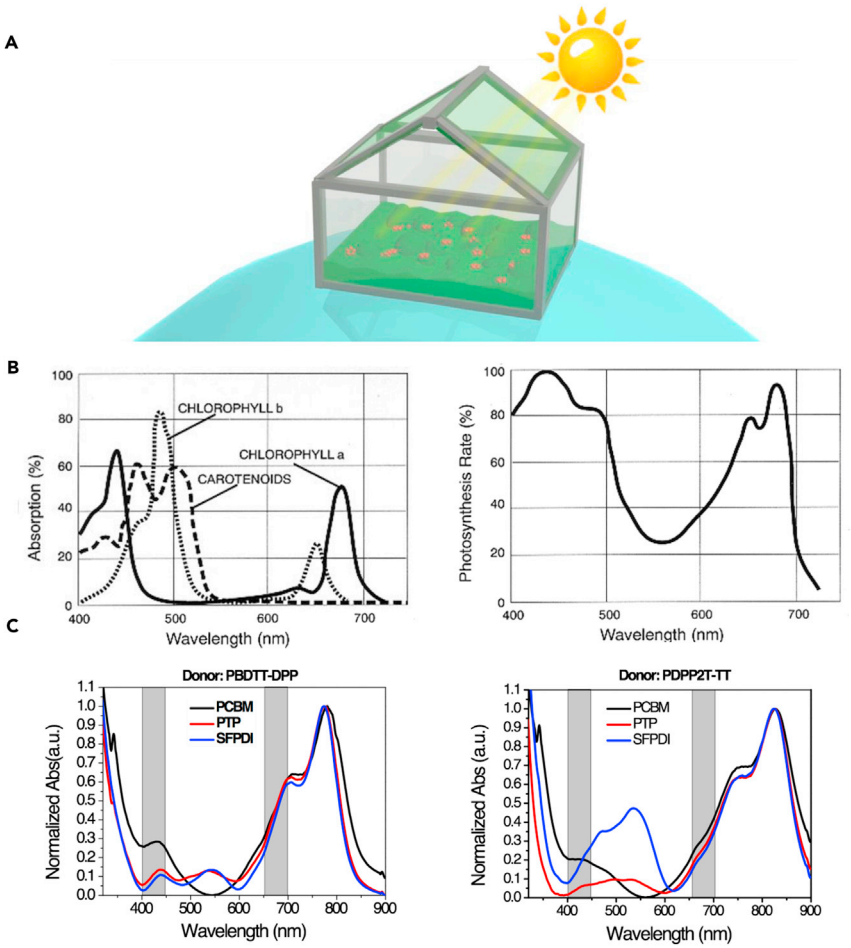

Figure 4. Application of Transparent Polymer Photovoltaics

(A) Schematic representation of a greenhouse embedded with spectrum-tunable organic photovoltaics on its roof for agricultural use.

(B) (Left) Absorption spectra for chlorophyll *a*, chlorophyll *b*, and carotenoids extracted in a solution. (Right) PAR action spectrum of an isolated chloroplast. This indicates that only a specific spectrum range is needed for the plant growth. Reprinted from Corrado et al.,[73] with permission. Copyright 1999, Springer Nature.

(C) Absorption spectra for (left) PBDTT-DPP and (right) PDPP2T-TT donors with PCBM, PTP, and SFPDI acceptors. The shaded areas (400–450 nm and 650–700 nm) indicate the peak absorption region of chlorophyll *a* for plant growth.

multiplication rate of algal cells is highest at a photon flux of 100 μmol m^{-2} s^{-1}, while the one-sun condition is equivalent to 2000 μmol m^{-2} s^{-1}, or about 20 times the light that algal biomass needs.[75] Therefore, for the growth of some plants, the greenhouse needs to be at least 50% transparent to allow light at least in the photon spectrum region used by these plants. However, for other organisms (e.g., algae), it may need to be only 10% transparent to allow light in the electromagnetic region used by such organisms. This means that for some specific plants there can be more sunlight spared for the OPV of the greenhouse to generate more electricity.

Consequently, PV devices can be designed to capture electromagnetic energy in regions of the spectrum that are not used, or used less predominantly, for photosynthesis and photomorphogenesis. For example, the 500- to 640-nm section within the

visible region is relatively marginal to plant use, which means that TOPV can be applied to generate additional power in the greenhouse. Therefore, the PV spectral response can be tuned to use that section of light as well and to maximize the total solar energy conversion efficiency.

Based on the previous description, a greenhouse consisting of a BIPV and a portion of the enclosed structure should have at least 10%–50% transparency to sunlight in the range 400–700 nm. To fulfill these requirements, new organic materials absorbent in IR and UV ranges are highly important. They can alter the absorption spectra through molecular design and are easily compatible with flexible substrates, while still retaining excellent visible regional transmittance and EQE compared with the inorganic PV systems. In other words, TOPV can facilitate active materials with complementary absorption to achieve efficient electricity generation and sufficient plant growth conditions at the same time. TOPV (700–1,000 nm) can reach a PCE of over 10%, achieving an efficient greenhouse with very high PCE BIPV.[76] Figure 4C shows the absorption spectra of currently available visibly transparent OPV materials. The transmission of the complete device in the visible range is above 50%, with the maximum transparency reaching 75%. This indicates that the TOPV by itself can indeed provide high, or almost full, transparency in the visible spectrum and harvest unused IR photons.

Summary and Outlook

Polymer PV are drawing more attention in the PV field because of the development of numerous novel materials and their consequent versatile applications. To make a successful transparent device, high efficiency, high transparency, and precision of color are all equally important. Research groups focus on three directions: photoactive material design, electrode design, and novel applications. Regarding the first aspect, the target is to simultaneously achieve high efficiency and maintain visible transparency, which can be done by shifting the material absorption spectrum to the IR region. The design of p-type D-A copolymers, which enables a separate control of LUMO and HOMO levels, has been found to successfully strengthen the absorbance and EQE in the IR region. The new n-type non-fullerene acceptors are also suitable for these emerging p-type materials and demonstrate good performance in the IR region. With regard to the second aspect, the goal of research on transparent electrode materials is to reduce the absorbance of the whole spectrum and maintain conductivity. PEDOT:PSS, thin silver, AgNW, 1D photonic crystal, and other carbon-based transporting layers have proved to be good candidates for transparent electrodes. Among these materials, the composite mirror layers, such as photonic crystal structures, are more favorable in TOPV because of their tunable reflection spectra that can control both the transmittance and color rendering. Regarding the third aspect, new and unique ideas concerning the further use of TOPV are being introduced. Studies on applications of TOPV are diverse, especially for spectrum-sensitive ones such as the BIPV in agriculture. Given the multifarious demand for light for organ growth and photosynthesis, TOPV are able to provide such an environment for developing the plants while generating additional power.

There are several key directions for further research on transparent polymer PV: (1) based on the ideas of shortening BLA and enhancing ICT, extension of the absorption region of organic materials beyond 1,000 nm can be realized; (2) by facilitating the IR absorption donor and acceptor units, photoactive materials can be constructed to limit absorbance of the active layer in the IR region; (3) to investigate the relationship between the V_{OC} loss and molecular structure; (4) to introduce novel transparent electrodes with both good conductivity and transparency such as

carbon-based compounds; (5) to utilize plasmonic effects, such as photonic crystals and patterned coatings on the device, to enhance the photon absorption in a specific region; (6) tuning the light field distribution through modifying the thicknesses of each layer in the device to achieve a higher CRI index. Research groups should also demonstrate methods of scalability to assist in technology transition from laboratory to industry, as well as to demonstrate TOPV prototypes in other applications such as agriculture, construction, automobiles, and aviation.

ACKNOWLEDGMENTS

Y.Y. acknowledges the Air Force Office of Scientific Research (AFOSR) (FA2386-15-1-4108, FA9550e15-1e0610, and FA9550-15-1-0333), Office of Naval Research (ONR) (N00014-14-1-0648 and N00014-04-1-0434), National Science Foundation (NSF) (ECCS-1509955), and UC-Solar Program (MRPI 328368) for their financial support. We also thank Dr. Dong Meng, Mr. Jun Yuan, Mr. Nicholas de Marco, Ms. Jingjing Xue, Ms. Selbi Nuryyeva, and Mr. Yuqiang Liu for providing important insights on this paper.

AUTHOR CONTRIBUTIONS

S.-Y.C. and P.C. investigated and wrote the original draft. G.L. and Y.Y. contributed to the conceptualization of spectrum-sensitive application of TOPV as well as reviewing and editing.

REFERENCES

1. Li, G., Zhu, R., and Yang, Y. (2012). Polymer solar cells. Nat. Photonics *6*, 153–161.

2. Dou, L., Liu, Y., Hong, Z., Li, G., and Yang, Y. (2015). Low-bandgap near-IR conjugated polymers/molecules for organic electronics. Chem. Rev. *115*, 12633–12665.

3. Lu, L., Zheng, T., Wu, Q., Schneider, A.M., Zhao, D., and Yu, L. (2015). Recent advances in bulk heterojunction polymer solar cells. Chem. Rev. *115*, 12666–12731.

4. Günes, S., Neugebauer, H., and Sariciftci, N.S. (2007). Conjugated polymer-based organic solar cells. Chem. Rev. *107*, 1324–1338.

5. Su, Y.-W., Lan, S.-C., and Wei, K.-H. (2012). Organic photovoltaics. Mater. Today *15*, 554–562.

6. Zhao, J., Li, Y., Yang, G., Jiang, K., Lin, H., Ade, H., Ma, W., and Yan, H. (2016). Efficient organic solar cells processed from hydrocarbon solvents. Nat. Energy *1*, 15027.

7. Sun, C., Pan, F., Bin, H., Zhang, J., Xue, L., Qiu, B., Wei, Z., Zhang, Z.-G., and Li, Y. (2018). A low cost and high performance polymer donor material for polymer solar cells. Nat. Commun. *9*, 743–752.

8. Renewable Resource Data Center. (2009). Reference solar spectral irradiance: ASTM G-173. http://rredc.nrel.gov/solar/spectra/am1.5/astmg173/astmg173.html.

9. Xu, G., Shen, L., Cui, C., Wen, S., Xue, R., Chen, W., Chen, H., Zhang, J., Li, H., Li, Y., and Li, Y. (2017). High-performance colorful semitransparent polymer solar cells with ultrathin hybrid-metal electrodes and fine-tuned dielectric mirrors. Adv. Funct. Mater. *27*, 1605908–1605917.

10. Li, G., Chu, C.-W., Shrotriya, V., Huang, J., and Yang, Y. (2006). Efficient inverted polymer solar cells. Appl. Phys. Lett. *88*, 253503.

11. Bailey-Salzman, R.F., Rand, B.P., and Forrest, S.R. (2006). Semitransparent organic photovoltaic cells. Appl. Phys. Lett. *88*, 233502.

12. Tai, Q., and Yan, F. (2017). Emerging semitransparent solar cells: materials and device design. Adv. Mater. *29*, 1700192–1700228.

13. Traverse, C.J., Pandey, R., Barr, M.C., and Lunt, R.R. (2017). Emergence of highly transparent photovoltaics for distributed applications. Nat. Energy *2*, 849–860.

14. Cheng, Y.-J., Yang, S.-H., and Hsu, C.-S. (2009). Synthesis of conjugated polymers for organic solar cell applications. Chem. Rev. *109*, 5868–5923.

15. Zhou, H., Yang, L., and You, W. (2012). Rational design of high performance conjugated polymers for organic solar cells. Macromolecules *45*, 607–632.

16. Zhang, Z.-G., and Li, Y. (2015). Side-chain engineering of high-efficiency conjugated polymer photovoltaic materials. Sci. China Chem. *58*, 192–209.

17. Su, Y.-W., Lin, Y.-C., and Wei, K.-H. (2017). Evolving molecular architectures of donor–acceptor conjugated polymers for photovoltaic applications: from one-dimensional to branched to two-dimensional structures. J. Mater. Chem. A. *5*, 24051–24075.

18. Wu, J.-S., Cheng, S.-W., Cheng, Y.-J., and Hsu, C.-S. (2015). Donor–acceptor conjugated polymers based on multifused ladder-type arenes for organic solar cells. Chem. Soc. Rev. *44*, 1113–1154.

19. Lunt, R.R. (2012). Theoretical limits for visibly transparent photovoltaics. Appl. Phys. Lett. *101*, 043902.

20. Reineke, S., Thomschke, M., Lüssem, B., and Leo, K. (2013). White organic light-emitting diodes: status and perspective. Rev. Mod. Phys. *85*, 1245–1293.

21. Chen, C.-C., Dou, L., Zhu, R., Chung, C.-H., Song, T.-B., Zheng, Y.B., Hawks, S., Li, G., Weiss, P.S., and Yang, Y. (2012). Visibly transparent polymer solar cells produced by solution processing. ACS Nano *6*, 7185–7190.

22. Dou, L., Chen, C.-C., Yoshimura, K., Ohya, K., Chang, W.-H., Gao, J., Liu, Y., Richard, E., and Yang, Y. (2013). Synthesis of 5H-Dithieno[3,2-b:2′,3′-d]pyran as an electron-rich building block for donor-acceptor type low-bandgap polymers. Macromolecules *46*, 3384–3390.

23. Zheng, Z., Zhang, S., Zhang, J., Qin, Y., Li, W., Yu, R., Wei, Z., and Hou, J. (2016). Over 11% efficiency in tandem polymer solar cells featured by a low-band-gap polymer with fine-tuned properties. Adv. Mater. *28*, 5133–5138.

24. Chen, C.-C., Dou, L., Gao, J., Chang, W.-H., Li, G., and Yang, Y. (2013). High-performance semi-transparent polymer solar cells possessing tandem structures. Energy Environ. Sci. *6*, 2714–2720.

25. Hendriks, K.H., Li, W., Wienk, M.M., and Janssen, R.A. (2014). Small-bandgap semiconducting polymers with high near-infrared photoresponse. J. Am. Chem. Soc. *136*, 12130–12136.

26. Lin, Y., Wang, J., Zhang, Z.G., Bai, H., Li, Y., Zhu, D., and Zhan, X. (2015). An electron acceptor challenging fullerenes for efficient polymer solar cells. Adv. Mater. *27*, 1170–1174.

27. Wang, W., Yan, C., Lau, T.K., Wang, J., Liu, K., Fan, Y., Lu, X., and Zhan, X. (2017). Fused hexacyclic nonfullerene acceptor with strong near-infrared absorption for semitransparent organic solar cells with 9.77% efficiency. Adv. Mater. *29*, 1701308–1701314.

28. Yao, H., Chen, Y., Qin, Y., Yu, R., Cui, Y., Yang, B., Li, S., Zhang, K., and Hou, J. (2016). Design and synthesis of a low bandgap small molecule acceptor for efficient polymer solar cells. Adv. Mater. *28*, 8283–8287.

29. Yao, H., Cui, Y., Yu, R., Gao, B., Zhang, H., and Hou, J. (2017). Design, synthesis, and photovoltaic characterization of a small molecular acceptor with an ultra-narrow band gap. Angew. Chem. Int. Ed. *56*, 3045–3049.

30. Huang, J., Li, G., and Yang, Y. (2008). A semi-transparent plastic solar cell fabricated by a lamination process. Adv. Mater. *20*, 415–419.

31. Chang, C.-Y., Zuo, L., Yip, H.-L., Li, Y., Li, C.-Z., Hsu, C.-S., Cheng, Y.-J., Chen, H., and Jen, A.K.Y. (2013). A versatile fluoro-containing low-bandgap polymer for efficient semitransparent and tandem polymer solar cells. Adv. Funct. Mater. *23*, 5084–5090.

32. Guo, F., Kubis, P., Stubhan, T., Li, N., Baran, D., Przybilla, T., Spiecker, E., Forberich, K., and Brabec, C.J. (2014). Fully solution-processing route toward highly transparent polymer solar cells. ACS Appl. Mater. Interfaces *6*, 18251–18257.

33. Betancur, R., Romero-Gomez, P., Martinez-Otero, A., Elias, X., Maymó, M., and Martorell, J. (2013). Transparent polymer solar cells employing a layered light-trapping architecture. Nat. Photonics *7*, 995–1000.

34. Chueh, C.C., Chien, S.C., Yip, H.L., Salinas, J.F., Li, C.Z., Chen, K.S., Chen, F.C., Chen, W.C., and Jen, A.K.Y. (2013). Toward high-performance semi-transparent polymer solar cells: optimization of ultra-thin light absorbing layer and transparent cathode architecture. Adv. Energy Mater. *3*, 417–423.

35. Colsmann, A., Puetz, A., Bauer, A., Hanisch, J., Ahlswede, E., and Lemmer, U. (2011). Efficient semi-transparent organic solar cells with good transparency color perception and rendering properties. Adv. Energy Mater. *1*, 599–603.

36. Chen, K.-S., Salinas, J.-F., Yip, H.-L., Huo, L., Hou, J., and Jen, A.K.-Y. (2012). Semi-transparent polymer solar cells with 6% PCE, 25% average visible transmittance and a color rendering index close to 100 for power generating window applications. Energy Environ. Sci. *5*, 9551–9557.

37. Yu, W., Jia, X., Long, Y., Shen, L., Liu, Y., Guo, W., and Ruan, S. (2015). Highly efficient semitransparent polymer solar cells with color rendering index approaching 100 using one-dimensional photonic crystal. ACS Appl. Mater. Interfaces *7*, 9920–9928.

38. Qu, S., and Tian, H. (2012). Diketopyrrolopyrrole (DPP)-based materials for organic photovoltaics. Chem. Commun. *48*, 3039–3051.

39. Wienk, M.M., Turbiez, M., Gilot, J., and Janssen, R.A. (2008). Narrow-bandgap diketo-pyrrolo-pyrrole polymer solar cells: the effect of processing on the performance. Adv. Mater. *20*, 2556–2560.

40. Huo, L., Hou, J., Chen, H.-Y., Zhang, S., Jiang, Y., Chen, T.L., and Yang, Y. (2009). Bandgap and molecular level control of the low-bandgap polymers based on 3,6-dithiophen-2-yl-2,5-dihydropyrrolo [3, 4-c] pyrrole-1,4-dione toward highly efficient polymer solar cells. Macromolecules *42*, 6564–6571.

41. Dou, L., You, J., Yang, J., Chen, C.-C., He, Y., Murase, S., Moriarty, T., Emery, K., Li, G., and Yang, Y. (2012). Tandem polymer solar cells featuring a spectrally matched low-bandgap polymer. Nat. Photonics *6*, 180–185.

42. Lin, Y.-C., Cheng, H.-W., Su, Y.-W., Lin, B.-H., Lu, Y.-J., Chen, C.-H., Chen, H.-C., Yang, Y., and Wei, K.-H. (2018). Molecular engineering of side chain architecture of conjugated polymers enhances performance of photovoltaics by tuning ternary blend structures. Nano Energy *43*, 138–148.

43. Chen, Z., Lemke, H., Albert-Seifried, S., Caironi, M., Nielsen, M.M., Heeney, M., Zhang, W., McCulloch, I., and Sirringhaus, H. (2010). High mobility ambipolar charge transport in polyselenophene conjugated polymers. Adv. Mater. *22*, 2371–2375.

44. Kong, H., Jung, Y.K., Cho, N.S., Kang, I.-N., Park, J.-H., Cho, S., and Shim, H.-K. (2009). New semiconducting polymers containing 3,6-dimethyl (thieno [3,2-b] thiophene or selenopheno [3,2-b] selenophene) for organic thin-film transistors. Chem. Mater. *21*, 2650–2660.

45. Kronemeijer, A.J., Gili, E., Shahid, M., Rivnay, J., Salleo, A., Heeney, M., and Sirringhaus, H. (2012). A selenophene-based low-bandgap donor–acceptor polymer leading to fast ambipolar logic. Adv. Mater. *24*, 1558–1565.

46. Dou, L., Chang, W.-H., Gao, J., Chen, C.-C., You, J., and Yang, Y. (2013). A selenium-substituted low-bandgap polymer with versatile photovoltaic applications. Adv. Mater. *25*, 825–831.

47. Li, G., Shrotriya, V., Huang, J., Yao, Y., Moriarty, T., Emery, K., and Yang, Y. (2005). High-efficiency solution processable polymer photovoltaic cells by self-organization of polymer blends. Nat. Mater. *4*, 864–868.

48. Mukherjee, S., Proctor, C.M., Bazan, G.C., Nguyen, T.-Q., and Ade, H. (2015). Significance of average domain purity and mixed domains on the photovoltaic performance of high-efficiency solution-processed small-molecule BHJ solar cells. Adv. Energy Mater. *5*, 1500877–1500887.

49. Richter, L.J., DeLongchamp, D.M., Bokel, F.A., Engmann, S., Chou, K.W., Amassian, A., Schaible, E., and Hexemer, A. (2015). In situ morphology studies of the mechanism for solution additive effects on the formation of bulk heterojunction films. Adv. Energy Mater. *5*, 1400975–1400985.

50. Liu, F., Gu, Y., Wang, C., Zhao, W., Chen, D., Briseno, A.L., and Russell, T.P. (2012). Efficient polymer solar cells based on a low bandgap semi-crystalline DPP polymer-PCBM blends. Adv. Mater. *24*, 3947–3951.

51. Lin, Y.-C., Su, Y.-W., Li, J.-X., Lin, B.-H., Chen, C.-H., Chen, H.-C., Wu, K.-H., Yang, Y., and Wei, K.-H. (2017). Energy transfer within small molecule/conjugated polymer blends enhances photovoltaic efficiency. J. Mater. Chem. A. *5*, 18053–18063.

52. Liao, S.H., Jhuo, H.J., Cheng, Y.S., and Chen, S.A. (2013). Fullerene derivative-doped zinc oxide nanofilm as the cathode of inverted polymer solar cells with low-bandgap polymer (PTB7-Th) for high performance. Adv. Mater. *25*, 4766–4771.

53. Zhao, W., Qian, D., Zhang, S., Li, S., Inganäs, O., Gao, F., and Hou, J. (2016). Fullerene-free polymer solar cells with over 11% efficiency and excellent thermal stability. Adv. Mater. *28*, 4734–4739.

54. Li, X., Huang, H., Bin, H., Peng, Z., Zhu, C., Xue, L., Zhang, Z.-G., Zhang, Z., Ade, H., and Li, Y. (2017). Synthesis and photovoltaic properties of a series of narrow bandgap organic semiconductor acceptors with their absorption edge reaching 900 nm. Chem. Mater. *29*, 10130–10138.

55. Li, X., Yan, T., Bin, H., Han, G., Xue, L., Liu, F., Yi, Y., Zhang, Z.-G., Russell, T.P., and Li, Y. (2017). Insertion of double bond π-bridges of A-D-A acceptors for high performance near-infrared polymer solar cells. J. Mater. Chem. A. *5*, 22588–22597.

56. Huang, H., Li, X., Zhong, L., Qiu, B., Yang, Y., Zhang, Z.-G., Zhang, Z., and Li, Y. (2018). High performance as-cast semitransparent polymer solar cells. J. Mater. Chem. A. *6*, 4670–4677.

57. Bronstein, H., Ashraf, R.S., Kim, Y., White, A.J.P., Anthopoulos, T., Song, K., James, D., Zhang, W., and McCulloch, I. (2011). Synthesis of a novel fused thiophene-thieno[3,2-b] thiophene-thiophene donor monomer and co-polymer for use in OPV and OFETs. Macromol. Rapid Commun. *32*, 1664–1668.

58. Lin, Y., Zhang, Z.-G., Bai, H., Wang, J., Yao, Y., Li, Y., Zhu, D., and Zhan, X. (2015). High-performance fullerene-free polymer solar cells with 6.31% efficiency. Energy Environ. Sci. *8*, 610–616.

59. Li, Y., Lin, J.-D., Che, X., Qu, Y., Liu, F., Liao, L.-S., and Forrest, S.R. (2017). High efficiency near-infrared and semitransparent non-fullerene acceptor organic photovoltaic cells. J. Am. Chem. Soc. *139*, 17114–17119.

60. Li, Y., Xu, G., Cui, C., and Li, Y. (2018). Flexible and semitransparent organic solar cells. Adv. Energy Mater. *8*, 1701791.

61. Ke, L., Lai, S., Liu, H., Peh, C., Wang, B., and Teng, J. (2012). Ultrasmooth silver thin film on PEDOT: PSS nucleation layer for extended surface plasmon propagation. ACS Appl. Mater. Interfaces *4*, 1247–1253.

62. Espinosa, N., García-Valverde, R., Urbina, A., and Krebs, F.C. (2011). A life cycle analysis of polymer solar cell modules prepared using roll-to-roll methods under ambient conditions. Sol. Energy Mater. Sol. Cells *95*, 1293–1302.

63. Kim, S., and Lee, J.-L. (2012). Design of dielectric/metal/dielectric transparent electrodes for flexible electronics. J. Photon. Energy *2*, 021215.

64. Lungenschmied, C., Dennler, G., Neugebauer, H., Sariciftci, S.N., Glatthaar, M., Meyer, T., and Meyer, A. (2007). Flexible, long-lived, large-

area, organic solar cells. Sol. Energy Mater. Sol. Cells *91*, 379–384.

65. Lechêne, B.P., Cowell, M., Pierre, A., Evans, J.W., Wright, P.K., and Arias, A.C. (2016). Organic solar cells and fully printed super-capacitors optimized for indoor light energy harvesting. Nano Energy *26*, 631–640.

66. Yang, Y. and Li, G. (2014). Transparent organic solar cells for agronomic applications.US Patent Application US20160013433A1.

67. Loik, M.E., Carter, S.A., Alers, G., Wade, C.E., Shugar, D., Corrado, C., Jokerst, D., and Kitayama, C. (2017). Wavelength-selective solar photovoltaic systems: powering greenhouses for plant growth at the food-energy-water nexus. Earth Future *5*, 1044–1053.

68. Nayak, S., and Tiwari, G. (2008). Energy and exergy analysis of photovoltaic/thermal integrated with a solar greenhouse. Energ. Build. *40*, 2015–2021.

69. Yano, A., Onoe, M., and Nakata, J. (2014). Prototype semi-transparent photovoltaic modules for greenhouse roof applications. Biosyst. Eng. *122*, 62–73.

70. Yang, F., Zhang, Y., Hao, Y., Cui, Y., Wang, W., Ji, T., Shi, F., and Wei, B. (2015). Visibly transparent organic photovoltaic with improved transparency and absorption based on tandem photonic crystal for greenhouse application. Appl. Opt. *54*, 10232–10239.

71. Allardyce, C.S., Fankhauser, C., Zakeeruddin, S.M., Grätzel, M., and Dyson, P.J. (2017). The influence of greenhouse-integrated photovoltaics on crop production. Sol. Energy *155*, 517–522.

72. Corrado, C., Leow, S.W., Osborn, M., Carbone, I., Hellier, K., Short, M., Alers, G., and Carter, S.A. (2016). Power generation study of luminescent solar concentrator greenhouse. J. Renew. Sustain. Energy *8*, 043502.

73. Whitmarsh, J., and Govindjee. (1999). The photosynthetic process. In Concepts in Photobiology: Photosynthesis and Photomorphogenesis, G.S. Singhal, G. Renger, S.K. Sopory, K.D. Irrgang, and Govindjee., eds. (Dordrecht, Netherlands: Springer), pp. 11–51.

74. Smith, H. (1994). Sensing the light environment: the functions of the phytochrome family. In Photomorphogenesis in Plants, R.E. Kendrick and G.H.M. Kronenberg, eds. (Dordrecht, Netherlands: Springer), pp. 377–416.

75. Al-Qasmi, M., Raut, N., Talebi, S., Al-Rajhi, S., and Al-Barwani, T. (2012). A review of effect of light on microalgae growth. Proc. World Congr. Eng. 608–610.

76. Dai, S., Li, T., Wang, W., Xiao, Y., Lau, T.K., Li, Z., Liu, K., Lu, X., and Zhan, X. (2018). Enhancing the performance of polymer solar cells via core engineering of NIR-absorbing electron acceptors. Adv. Mater. https://doi.org/10.1002/adma.201706571.